Materials and Design 45 (2013) 487–496

Contents lists available at SciVerse ScienceDirect

Materials and Design

journal homepage: www.elsevier.com/locate/matdes

Mechanical and structural behavior of a swelling elastomer under compressive loading

Sayyad Zahid Qamar *, Maaz Akhtar, Tasneem Pervez, Moosa S.M. Al-Kharusi

Mechanical and Industrial Engineering Department, Box 33, Sultan Qaboos University, Al Khoudh 123, Oman

ARTICLE INFO

Article history:
Received 12 July 2012
Accepted 11 September 2012
Available online 21 September 2012

Keywords:
Swelling elastomer
Compression testing
Bulk testing
Numerical simulation
Mechanical response
Structural behavior

ABSTRACT

Swelling elastomers are a new breed of advanced polymers, and over the last two decades they have found increasing use in drilling of difficult oil and gas wells, remediation of damaged wells, and rejuvenation of abandoned wells. It is important to know whether an elastomer type or a certain seal design will function properly and reliably under a given set of oil or gas well conditions. This paper reports the results of an experimental and numerical study conducted to analyze how compressive and bulk behavior of an actual oilfield elastomer changes due to swelling. Tests were carried out on ASTM-standard compression and bulk samples (discs) before swelling and after different swelling periods. Elastic and bulk modulii were experimentally determined under different swelling conditions. Shear modulus and Poisson's ratio were estimated using derived isotropic relations. Cross-link chain density and number average molecular weight were obtained using predictive equations of polymer physics. Mechanical testing was also modeled and simulated using the nonlinear finite element package ABAQUS, material model being Ogden hyperelastic model with second strain energy potential.

Values of elastic and shear modulus dropped by more than 90% in the first few days, and then remained almost constant during the rest of the 1-month period. Poisson's ratio, as expected, showed a mirror behavior of a sharp increase in the first few days. Bulk modulus exhibited a fluctuating pattern; rapid initial decrease, then a slightly slower increase, followed by a much slower decrease. Salinity shows some notable effect in the first 5 or 6 days, but has almost no influence in the later days. As swelling progresses, chain density decreases, much more sharply in the first week and then showing almost a steady-state behavior. In contrast, cross-link average molecular weight increases with swelling (as expected), but in a slightly fluctuating manner. Very interestingly, Poisson's ratio approaches the limiting value of 0.5 within the first 10 days of swelling, justifying the assumption of incompressibility used in most analytical and numerical models. In general, simulations results are in good agreement with experimental ones. Results presented here can find utility in selection of swelling elastomers suitable for a given set of field conditions, in improvement of elastomer-seal and swell-packer design, and in modeling and simulation of seal performance.

1. Introduction

Many new and ground-breaking technologies are closely associated with advances made in the area of materials science and engineering. Swelling elastomer, a recently developed advanced polymer, is an apt example. Elastomers are highly elastic rubber-like materials that can stretch up to 500% of their original length [1]. Swelling elastomers swell when they interact with fluids like water or oil [2]. Swelling results in changes in volume, thickness, density, hardness and mechanical properties [3,4]. Swelling rate for a specific elastomer depends on the temperature and composition of the swelling medium. Water-swelling elastomers swell through absorption of saline water following the mechanism of osmosis, while oil-swelling elastomers swell by absorption of hydrocarbons through a diffusion process [5]. Elastomers have low modulus of elasticity (E) ranging from 10 MPa to 4 GPa (E-value for most metals is in the 50–400 GPa range), but very high elongation reaching up to 1000% (elongation for metals is always less than 100%).

Maintaining the profitability of old wells and economically exploiting new reservoirs (that were previously inaccessible) are two of the main challenges facing the oil and gas industry. Also, zonal isolation and optimization of the hole-size with economic production for both conventional and deep water wells are ongoing problems [6,7]. Swelling elastomers have found extensive use in highly sophisticated new well applications where other materials fail to work [8]. Their successful applications include solution of drilling problems in deep shelf high-pressure high-temperature

* Corresponding author. Tel.: +968 24141349; fax: +968 24141316.
E-mail address: sayyad@squ.edu.om (S.Z. Qamar).

0261-3069/$ - see front matter © 2012 Elsevier Ltd. All rights reserved.
http://dx.doi.org/10.1016/j.matdes.2012.09.020

Nomenclature

E	Elastic/Young's modulus (N/m^2)	N	chain density (mol/cm^3)
K	bulk modulus (N/m^2)	M_C	number average chain molecular weight (g/mol)
G	shear modulus (N/m^2)	k	Boltzmann constant (J/K)
ν	Poisson's ratio	T	absolute temperature (K)
σ	engineering stress (N/m^2)	n	number of crosslink chains
ε	engineering strain (normal)	m	mass (kg)
γ	engineering strain (shear)	V	volume (m^3)
τ	shear stress (N/m^2)	ρ	density (kg/m^3)
p	hydrostatic stress (N/m^2)	R	general gas constant (J/K-mol)
δ	volume dilatation (cm^3)	N_A	Avogadro's number (#/mol)

(HP/HT) wells [9]; use in conjunction with expandable tubular technology (SET) for improved well production [10,11]; water shutoff and other types of zonal isolation [12]; use in horizontal wells and in tandem with coiled tubing for better reservoir management [13,14]; optimization of multizone fractured wellbores [15]; etc.

Investigation of the swelling and mechanical behavior of these elastomers is essential in resolving application and design issues. When an elastomer seal is positioned in the well, environmental conditions initiate the swelling and the material may continue to swell throughout its life. Swelling results in the alteration of mechanical properties and sealing response. If elastomer seals are put into use without thoroughly studying these changes, resulting seal failure may cause loss of time, money, and other resources. Rework is not only time consuming but at times not possible at all. Failures may even cause the oil or gas production from the well to stop.

One critical aspect of good design is appropriate material selection. This cannot be done without reliable knowledge of how the material will behave when exposed to different loads, temperatures, and other environmental conditions. As swelling elastomers are basically used as sealing elements in petroleum applications, and as seals are under compressive loading, investigation of the mechanical behavior of elastomers under compression is very important.

Contemporary elastomer seal design is usually based on laboratory tests and trial-and-error method. To test all possible combinations of field parameters (elastomer material, water salinity, oil type, temperature, pressure, etc.) in the laboratory is almost impossible, especially for extended swelling periods. Numerical modeling and simulation of seal design, validated by experimental results, may provide answers for all possible scenarios, which cannot be attempted experimentally. Numerical simulations (FEM based, for example) can shorten the lead time for development of robust sealing applications in difficult or new oil and gas wells, offering an accurate and cost effective alternative to extensive testing.

This paper discusses four key mechanical properties of swelling elastomers (elastic modulus E, bulk modulus K, shear modulus G, and Poisson's ratio ν) and two polymer characteristics (cross-link chain density N, and average molecular weight M_C) needed for design improvement and performance analysis of elastomer seals. These parameters were experimentally determined for an elastomer being currently used by the petroleum industry, before and after various stages of swelling. To strengthen the experimental results, compression and bulk tests were also simulated using a commercial FEM package. After rigorous evaluation, the most appropriate hyperelastic material model (currently available in FEM packages) was used for these simulations. Simulation results are generally in good agreement with experimental values.

2. Theoretical background

As mentioned above, the paper discusses the effect of swelling on four mechanical properties that describe the macroscopic-level behavior of the elastomer, and on two microscopic-level characteristics that are related to polymer structure. Brief theoretical background and inter-relationships of these quantities are presented in this section.

2.1. Macroscopic behavior: isotropic relationships

Once the values of E and K are established experimentally, shear modulus (G) and Poisson's ratio (ν) can be determined using the isotropic relations derived below. The elastic behavior of any isotropic material is completely described by Hooke's law [16]:

$$\varepsilon_x = \frac{1}{E}[\sigma_x - \nu(\sigma_y + \sigma_z)], \quad \varepsilon_y = \frac{1}{E}[\sigma_y - \nu(\sigma_z + \sigma_x)], \quad \varepsilon_z = \frac{1}{E}[\sigma_x - \nu(\sigma_z + \sigma_y)], \tag{1}$$

where σ is the engineering stress and ε is the strain. Being in the elastic region, engineering shear strain (γ) is obviously proportional to shear stress (τ):

$$\gamma_{yz} = \frac{1}{G}\tau_{yz}, \quad \gamma_{zx} = \frac{1}{G}\tau_{zx}, \quad \gamma_{xy} = \frac{1}{G}\tau_{xy}. \tag{2}$$

Fig. 1 shows a body under a state of pure shear and its Mohr circle representation giving the principal stresses:

$$\sigma_1 = \tau_{xy} \quad \sigma_2 = -\tau_{xy} \quad \sigma_3 = 0 \quad \tau_{12} = 0. \tag{3}$$

We can use Eq. (1) (Hooke's law) to find the principal strains:

$$\varepsilon_1 = \frac{\tau_{xy}(1+\nu)}{E}, \quad \varepsilon_2 = \frac{\tau_{xy}(1+\nu)}{E}. \tag{4}$$

Shear strain γ_{xy} can also be expressed in terms of the principal strains:

$$\gamma_{xy} = \varepsilon_1 - \varepsilon_2 = \frac{2\tau_{xy}(1+\nu)}{E}. \tag{5}$$

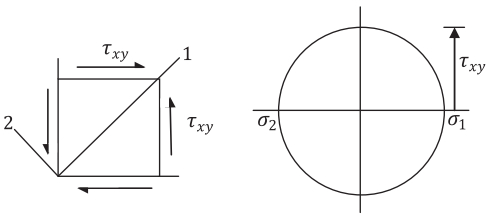

Fig. 1. A body under a state of pure shear, and its Mohr circle representation.

Comparing Eqs. (2) and (5), shear modulus becomes

$$G = \frac{E}{2(1+\nu)}. \tag{6}$$

For determination of bulk modulus (K), we need to consider the volume dilatation (volumetric strain) $\delta = \Delta V/V$ and the hydrostatic stress $-p = \frac{1}{3}(\sigma_x + \sigma_y + \sigma_z)$, giving

$$\delta = \frac{-p}{K}. \tag{7}$$

For a body undergoing linear strains, it can be easily shown that

$$\frac{dV}{V} = d\varepsilon_x + d\varepsilon_y + d\varepsilon_z. \tag{8}$$

This in turn yields

$$\delta = \varepsilon_x + \varepsilon_y + \varepsilon_z. \tag{9}$$

Comparing this result with Eq. (1), and simplifying, we get

$$\delta = \left(\frac{1-2\nu}{E}\right)(\sigma_x + \sigma_y + \sigma_z). \tag{10}$$

Recalling the definition of hydrostatic pressure p, and comparing with Eq. (7), we obtain the relationship between bulk modulus and Poisson's ratio

$$K = \frac{E}{3(1-2\nu)}. \tag{11}$$

Eqs. (6) and (11) have been used in this work to find the values of shear modulus and Poisson's ratio for the elastomeric material under study.

2.2. Structural behavior

2.2.1. Chain density

For any rubber-like material, network strands are formed both by cross-linking and molecular entanglement. As the degree of cross-linking increases, the cross-link chain density increases, making the elastomer more rigid, ultimately giving higher values of stiffness and shear modulus G [17]. Chain density can therefore be used as a measure of the swelling capability of an elastomer. For elastomers subjected to small strains, shear modulus is directly related to the number of cross-link chains per unit volume (chain density) N:

$$G = NkT, \tag{12}$$

where k is the Boltzmann's constant, and T is the temperature in Kelvin.

2.2.2. Number average chain molecular weight

Length of the network chains decreases due to an increase in the degree of cross-linking. In any polymer, chain density is closely related to the average molecular weight, and this property can also be used to explain the mechanics of swelling [18]. Multiplying and dividing Eq. (12) by Avogadro's number N_A, and recalling that $R = N_A k$, we can obtain

$$G = NRT/N_A, \tag{13}$$

If n is the number of chains, Avogadro's number can also be written as

$$N_A = nM_C/m. \tag{14}$$

Combining the definition of chain density ($N = n/V$) with Eq. (14) yields

$$N/N_A = \rho/M_C. \tag{15}$$

Comparing this result with Eq. (13), we get the expression for the number average chain molecular weight

$$M_C = \rho RT/G. \tag{16}$$

Once the values of shear modulus G are determined experimentally, these structural properties of the elastomer (N and M_C) can be easily evaluated using Eqs. (12) and (16) and their behavior due to swelling can be studied.

3. Experimental work

3.1. Swelling test

To replicate actual field conditions in many regional oil wells, samples of a water-swelling elastomer (used in various petroleum development applications) were subjected to swelling in saline water of 0.6% (6.000 ppm) and 12% (120,000 ppm) concentration maintained at a temperature of 50 °C. To investigate the effect of swelling, samples were taken out for mechanical testing after 1, 2, 4, 7, 10, 16, 23, and 30 days of swelling. The elastomer was a fast-swell type, so readings were initially taken after almost each day, and later on a weekly basis. Density is calculated from mass and volume measurements of each sample.

3.2. Mechanical testing

Two types of experiments have been performed to determine relevant material parameters: compression tests for Young's modulus (E), and bulk tests for bulk modulus (K). Compression and bulk tests are performed on elastomer samples before swelling, and are repeated after various stages of swelling over the 1-month test period. As elastomers in all sealing applications are under compression, Young's modulus determined through compression testing is the more relevant parameter, therefore behavior under tensile loading has not been studied.

Various researchers have investigated the behavior of rubber-like materials under compression [19], but not for swelling elastomers. For this study, ASTM standard test method (ASTM: D575) is followed during compression testing. As no standard is available for bulk testing of elastomers, a special test rig is used for bulk experiments, designed and fabricated in-house. Both compression and bulk tests use disc samples. As discs undergo significant volume change due to swelling, specimen dimensions are reworked (trimmed) prior to mechanical testing in order to match the ASTM standard. To ensure repeatability and consistency, all reported values are average of readings from three samples.

3.3. Sample preparation

Disc samples were cut using a die-and-punch set, with some surface grinding needed for final trimming. As prescribed by ASTM: D575, disc dimensions for compression testing are 28.6 mm diameter and 12.5 mm thickness. Due to reasons of confidentiality, actual identification number of swelling-elastomer material is not mentioned.

3.4. Compression testing

Compression tests are performed on a Tinius Olsen universal testing machine in the compression mode, using a 50-kN load cell; Fig. 2. Disc specimen is placed on a fixed bottom plate while the top plate applies a compressive load on the specimen. Elastomer sample is free to expand in the radial direction. Top surface of the disc moves downward with the compression load, while bottom surface is not allowed to move in the axial direction. Load is applied at a rate of 12 mm/min (ASTM: D575) until the specimen thickness is compressed to 10 mm. Force–deformation and

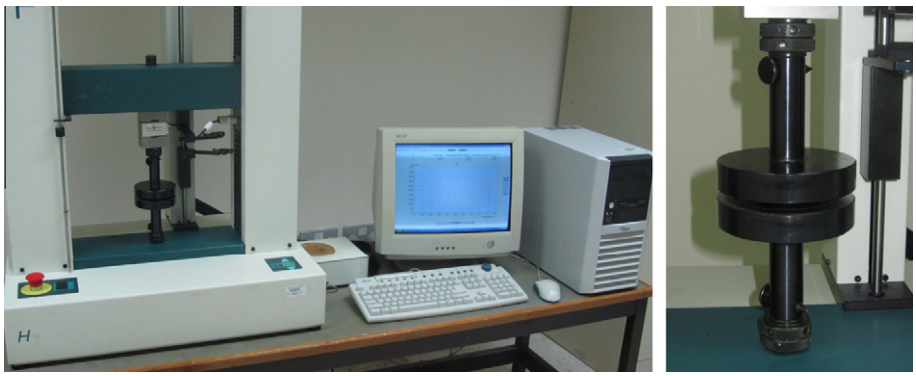

Fig. 2. Experimental setup for compression testing.

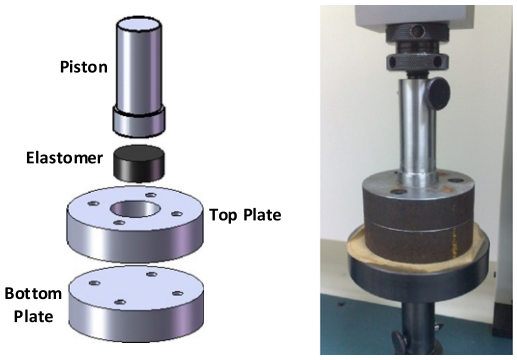

Fig. 3. Designed and fabricated test rig for bulk experiments.

stress–strain data are recorded. A small barreling effect can be observed in the compressed sample.

3.5. Bulk testing

The test rig that was designed and fabricated in-house for bulk testing is shown in Fig. 3. The rig is designed in such a way that under compressive loading the specimen is constrained to move only in the axial direction (no radial expansion allowed). To match with compression testing, load is applied at the rate of 12 mm/min until the specimen fails. Force–deformation results are recorded and later converted into pressure–volumetric strain data.

3.6. Numerical investigation

FEM-based numerical simulation has been done to lend strength to experimental results. Just as in experiments, simulations are run before swelling and after every swelling period. The commercial finite element package ABAQUS is used for all modeling and simulation work. Swelling elastomer specimen is modeled using 8-noded linear brick element with reduced integration (C3D8R). As mentioned above, Ogden hyper-elastic material model [20] with second strain energy potential is used for all simulations since it gives the closest results [21]. Coefficients for the material model are extracted (internally by the software) for all simulations from the experimental stress–strain data and values of Poisson's ratio and density.

3.7. Simulation of compression test

ASTM standard disc geometry is modeled for simulation of compression tests. Deformed and undeformed geometry is shown in Fig. 4. Same compressive loads and boundary conditions are applied as in the experiments. Simulations are conducted before swelling and after each swelling period (total 1 month period) under both salinity conditions. For each simulation, material properties are extracted from the experimental results. Stress–strain curves are plotted based on the simulation results.

3.8. Simulation of bulk test

Same sample geometry is modeled as in compression simulations, but the boundary conditions are different for simulation of bulk behavior. Disc is still under compression but restricted from movement in any direction. Only the top surface can move downward (z-axis) under the compressive load; Fig. 5. Same number of simulations is run as in the case of compression, for both the salinities. Simulation results are used to plot graphs of pressure against volumetric strain.

4. Results and discussion

All reported values from experimental work are average of readings taken from three samples. Stress–strain graphs are plotted for each of the compression tests. A 3-sample graph for one case (0.6% salinity, 30 days of swelling) is shown in Fig. 6. As discussed by Gent [17], only the initial 10% data from a stress–strain curve should be used to determine the Young's modulus for rubber-like materials. This small-strain approach has been followed in this work, guaranteeing the best straight-line fit, giving a maximum variation of 8% from the true modulus. Bulk modulus is determined by fitting a straight line to the linear portion of the pressure vs volumetric strain curve. A 3-sample graph is shown in Fig. 7 for elastomer exposed to 12% salinity, after 23 days of swelling. Regression for both elastic and bulk moduli shows a goodness of fit of more than 99%. Sample density is determined from mass and volume readings. Shear modulus and Poisson's ratio are calculated from experimental values of elastic and bulk modulus using isotropic relations for elastic materials (Eqs. (6) and (11)). Chain density and average molecular weight are determined through polymer structure relations (Eqs. (12) and (16)).

4.1. Effect of swelling on material behavior

Stress–strain graphs under compression (Fig. 6) exhibit significant non-linear behavior (as expected for elastomers). Samples of linear curve fitting to stress–strain data (first 10% of the data only, as explained above) and linear portion of bulk data are shown in Figs. 8 and 9 for extraction of the elastic and bulk modulii, respectively. A very high goodness of fit of 99.7% is quite reassuring. Fig. 10 shows stress–strain behavior before swelling and after 1,

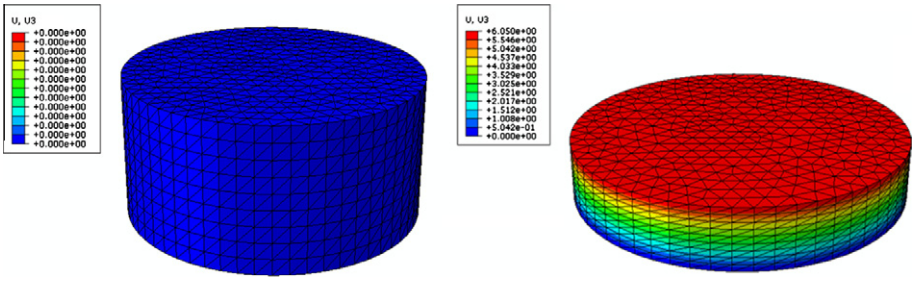

Fig. 4. Finite element model of compression test specimen; undeformed and deformed states.

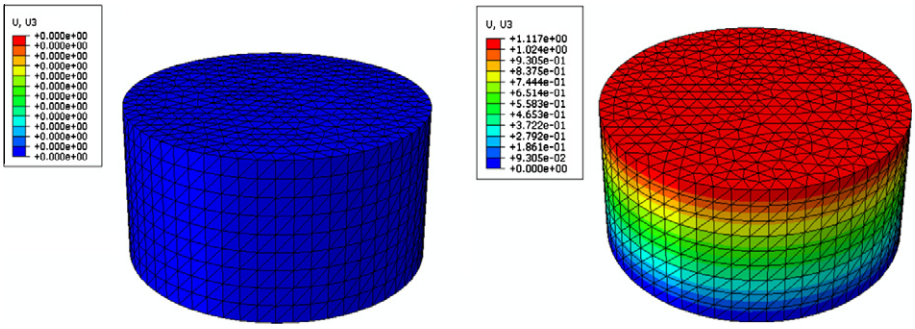

Fig. 5. Finite element model of bulk test specimen; undeformed and deformed states.

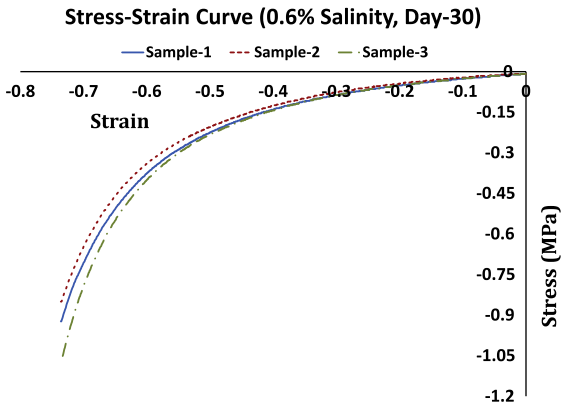

Fig. 6. Three-sample stress–strain curves for compression experiment; 0.6% salinity; 30 days of swelling.

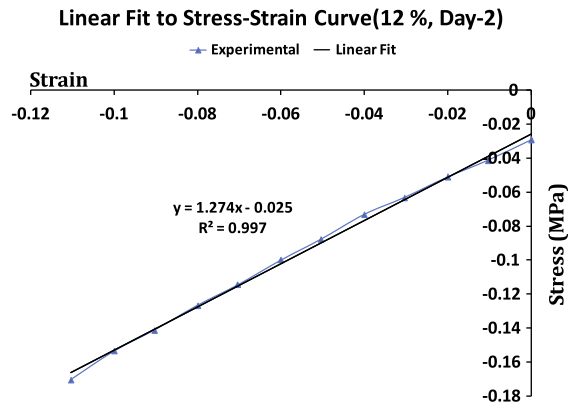

Fig. 8. Linear curve fitting to experimental stress–strain data; 12% salinity; 2 days of swelling.

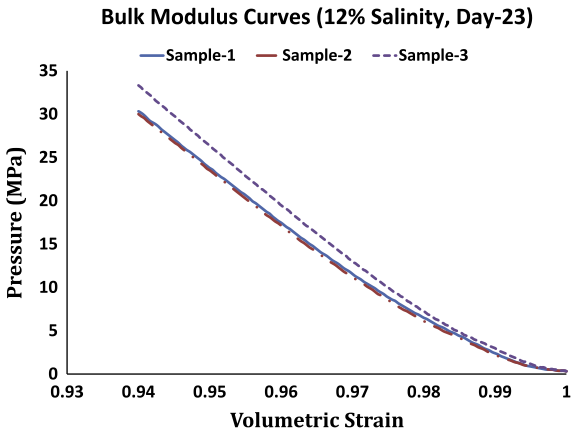

Fig. 7. Three-sample pressure–strain (volumetric) curves for bulk test; 12% salinity; 23 days of swelling.

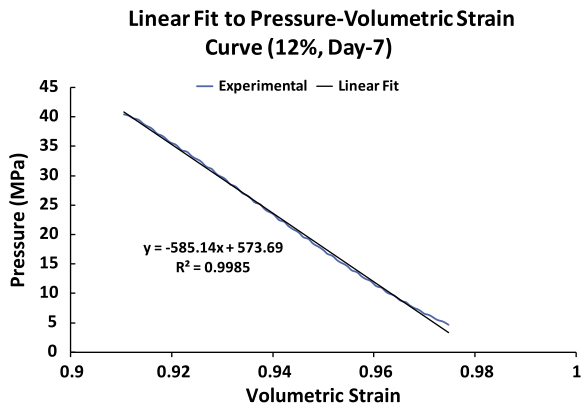

Fig. 9. Linear curve fitting to experimental data of pressure vs volumetric strain; 12% salinity; 7 days of swelling.

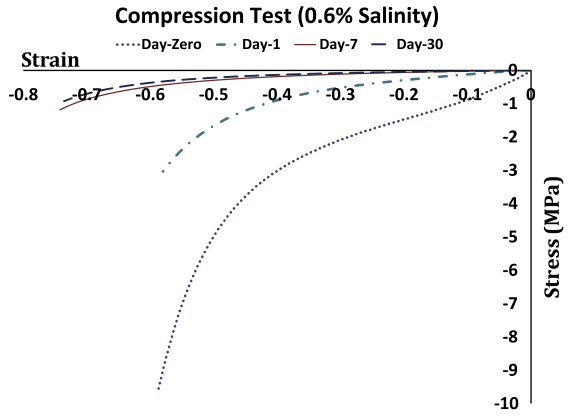

Fig. 10. Stress–strain behavior before swelling and after 1, 7, and 30 days of swelling.

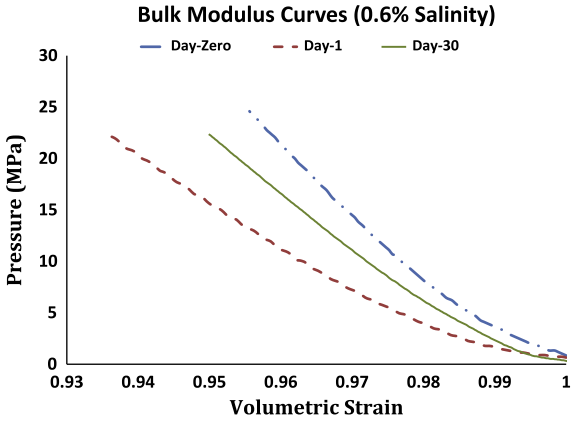

Fig. 11. Pressure vs volumetric–strain behavior before swelling and after 7 and 30 days of swelling.

7 and 30 days of swelling. It can be easily observed that compressive stress values decrease sharply after 1 day of swelling, and a little less noticeably at the end of the first week (day-7). After that there is hardly any change for the rest of the 1-month swelling period. Similarly, Fig. 11 shows the variation of pressure against volumetric strain (volume dilatation) before swelling and after specific swelling times. We again observe a sharper decrease in the early days, and a much slower variation in the later stages of swelling. This behavior is due to the fast-swell nature of this elastomer type

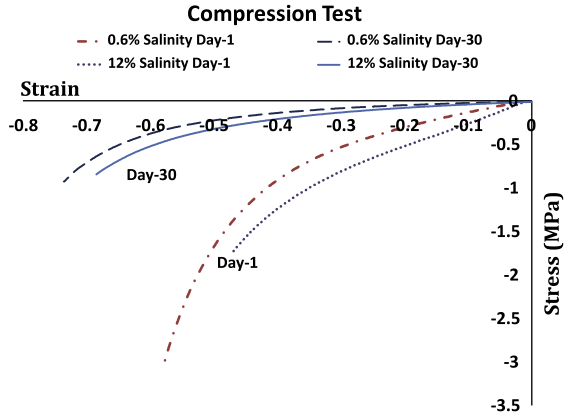

Fig. 12. Stress–strain behavior for the two salinities after 1-day and 30-days of swelling.

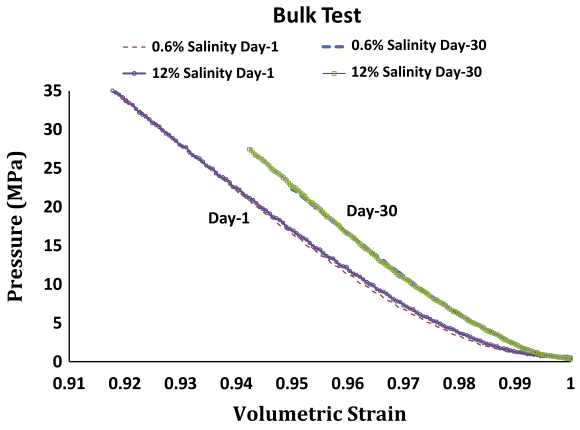

Fig. 13. Pressure–volumetric strain behavior for the two salinities after 1-day and 30-days of swelling.

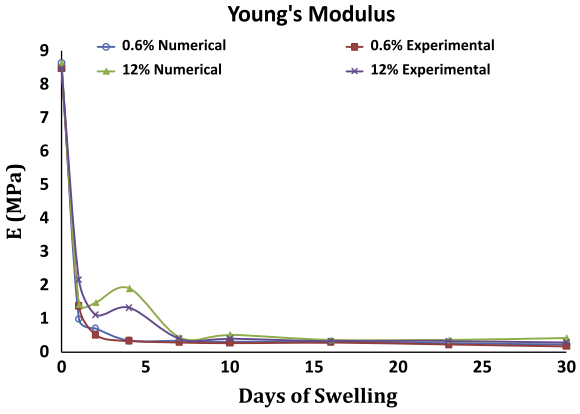

Fig. 14. Experimental and numerical results for Young's modulus under both salinities for the full 30-day test period.

(swelling rate very high in the first few days, then slowing down gradually). Engineering the elastomer in this way is intended to provide good sealing early on in petroleum development applications, so that the rig can go into production quickly. Higher amount of swelling makes the elastomer softer, resulting in large strains at much lower loads, thus the trend [2].

Figs. 12 and 13 illustrate stress–strain and pressure–volumetric strain behavior for the two salinities after 1-day and 30-days of swelling. It can be seen that stress (or pressure) values are higher for 12% salinity as compared to 0.6% (though only marginally), but become almost identical with more swelling. As expected, it is a consistent observation that these elastomers swell more when exposed to lower-salinity brine, since more concentrated solutions would not swell the elastomer as much as the diluted solutions, whether swelling happens due to diffusion or due to osmosis [4]. Under 12% salinity elastomer swells by a lesser amount, and the harder samples need larger stress to deform and fracture. With longer swelling period, amount of swelling under both salinities becomes roughly the same, thus the samples break at near-identical loads.

The following graphs show both experimental and simulation results for the full 30-day test period for different material parameters.

4.2. Variation of elastic modulus

As shown in Fig. 14, value of Young's modulus drops by more than 90% in the first few days, and then remains nearly constant

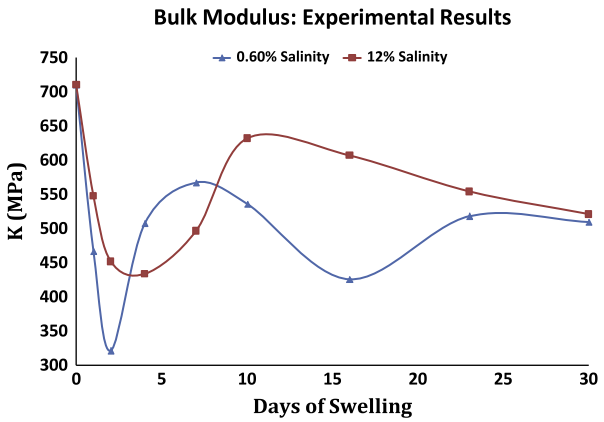

Fig. 15. Variation of bulk modulus over the 30-day swelling period; 0.6% and 12% salinity.

during the rest of the 1-month swelling period. For swelling under 12% salinity solution, *E*-value drops sharply in the first 2 days, and then increases a little before dropping down again. The overall trend is in line with stress–strain behavior explained above; very high swelling rate in the beginning, then a slow gradual change; thus a sharp initial drop in elasticity, followed by almost no change for longer swelling periods. The fluctuating pattern under higher-salinity solution may have roots in the nature of the swelling process [21]. It is known that salt is a constituent material for swelling elastomers. As the elastomer samples are exposed to salt solutions, some salt enters inside the elastomer as water is absorbed. On the other hand, small amounts of salt also break away from the elastomer and go into the salt solution. Due to this two-way transport, swelling does not happen in a constantly increasing fashion, but stops or slightly decreases for small intervals of time before increasing again. Apart from the constituent materials (including salt), another important factor in such elastomers is the cross-link chains. When some salt particles break away from the elastomer, the cross-links may be disturbed. This breaking and later re-forming of the cross-link chains may also affect whether swelling will increase or slightly decrease at a particular time. This fluctuation will obviously be more notable when the salt content in the brine is higher, thus the increasing–decreasing pattern of *E*-value under 12% salinity in Fig. 14.

4.3. Variation of bulk modulus

Variation of pressure against volumetric strain (under one condition and at any specific swelling period) shows a near-linear behavior (Fig. 7), making it easy to determine the bulk modulus. However, over the 30-day swelling period, bulk modulus exhibits a notable fluctuating pattern (Figs. 15 and 16): rapid initial decrease, then a slightly slower increase, followed by a much slower decrease. Values are generally higher in the case of 12% salinity. However, at the end of the 1-month swelling period, both salinities give almost the same modulus value. Apart from the reasons for fluctuation discussed above [2,4], significant oscillation in *K*-value may be rationalized from another perspective. During the compression test, sample elastomer disc is compressed in the axial direction, but is free to expand in the radial direction. However, in the bulk test, the disc specimen is constrained inside a cylinder so that there is only a uniaxial compression, with no radial expansion. In effect, this means that the elastomer behavior changes from incompressible (compression test) to compressible (bulk test). As all isotropic and other relations for rubbers and elastomers [17,18] are based on the assumption of incompressibility, this forced change to compressible behavior may also lead to notable deviation from regular trends.

4.4. Variation of Poisson's ratio

Exhibiting a mirror behavior in comparison with elastic modulus, Poisson's ratio increases sharply in the first few days, and then becomes constant for the remaining swelling period; Fig. 17. Young's modulus is related to deformation in the direction of applied load, while Poisson's ratio describes lateral deformation [16,18], thus the opposite trend of ν vs E is as expected. In the beginning, the two salinities yield slightly different values of ν, which become more or less the same after 10 days. During days 2–5, same pattern of fluctuation is observed (under 12% salinity) in Poisson's ratio as in the *E*-value, due to the swelling nature of the elastomer discussed above [2,4]. Moreover, it is interesting to note that ν approaches the limiting value of 0.5 within the first 10 days of swelling (for both salinities). This means that the assumption of incompressibility used in most analytical and numerical models of rubber-like materials [17,18] is also justified for swelling elastomers, given a reasonably large swelling period.

4.5. Variation of shear modulus

Just like Young's modulus, value of shear modulus drops by more than 90% in the first 5–6 days, and then remains practically constant during the rest of the swelling period; Fig. 18. Also, after the first few days, both salinities show the same values. More fluctuation under 12% salinity is also observed during days 2–7, owing to identical reasons [2,4].

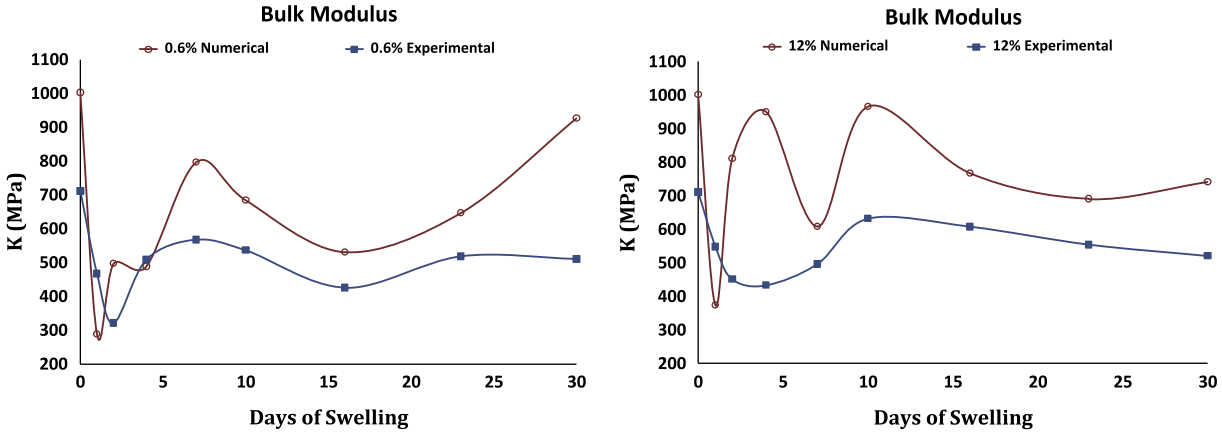

Fig. 16. Experimental and numerical results for bulk modulus for the full 30-day test period; 0.6% and 12% salinity.

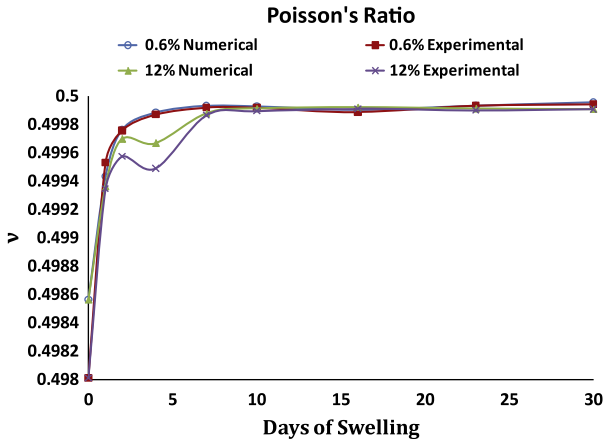

Fig. 17. Experimental and numerical results for Poisson's ratio under both salinities for the full 30-day test period.

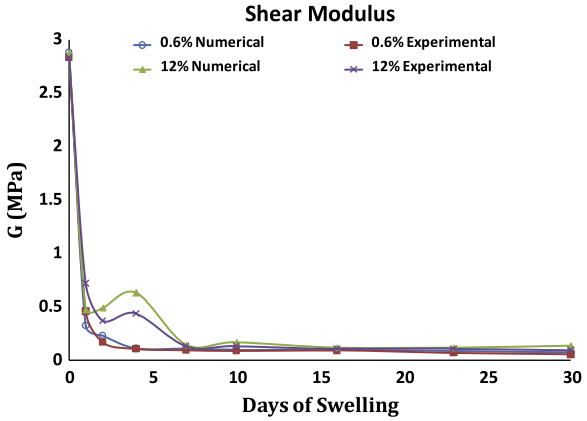

Fig. 18. Experimental and numerical results for shear modulus under both salinities for the full 30-day test period.

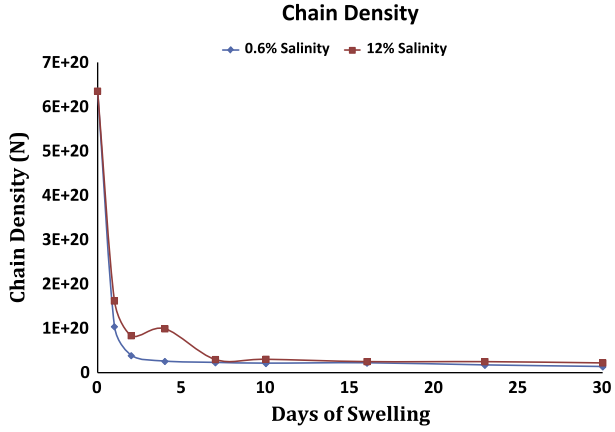

Fig. 19. Variation of chain density against swelling period under both salinities.

4.6. Variation of chain density

Variation in cross-link chain density (N) against amount of swelling (swelling period) is plotted in Fig. 19. Chain density drops drastically during the first few days, and then becomes nearly steady state. During days 2–7, N is higher for higher-salinity (12%) solution, otherwise response under both salinities is almost the same. As explained above, decrease in number of chains or cross-linking density (occurring here due to swelling) will make the elastomer softer [2,4,21], thereby contributing to a decrease in stiffness, elastic modulus, and rigidity (shear modulus). This change in polymer structure due to swelling is a direct explanation of the variation pattern observed in the mechanical properties.

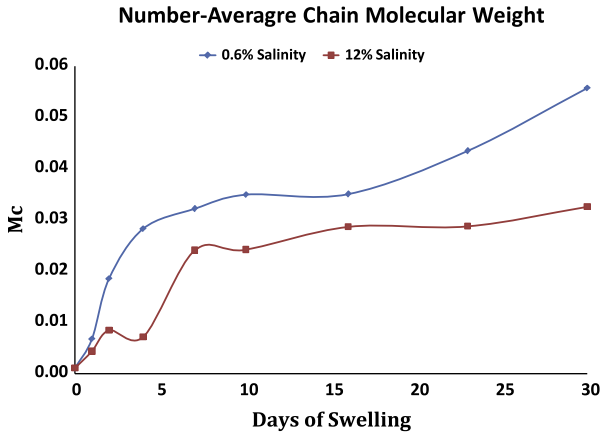

Fig. 20. Variation of average molecular weight against swelling period under both salinities.

4.7. Variation of number-average chain molecular weight

Fig. 20 shows the variation in number-average chain molecular weight (M_C) against swelling time over the 30-day test period. This average molecular weight of cross-link chains shows an overall increasing behavior with higher swelling amount, but with a somewhat fluctuating pattern; a much sharper increase in the first ten days or so, and then a slightly slower increase. It can be clearly seen from Eqs. (12) and (16) [17,18] that N and M_C are inversely related, so an increase of average molecular weight with swelling as against a corresponding decrease in chain density should be expected. As for fluctuation, the various reasons discussed above (including two-way transport of salt, forming and breaking of cross-link chains, etc.) are equally applicable in explanation of the observed variation in average molecular weight [2,4].

4.8. Comparison of experimental and numerical results

Overall there is very good agreement between experimental and simulation results. Stress–strain plots in the 10% strain region for experimental and numerical results of the compression test for one case (12% salinity, 23 days of swelling) are shown in Fig. 21, verifying the close conformity between test and simulation results.

Over the 30-day swelling period Young's modulus, Poisson's ratio, and shear modulus show almost perfect match between experimental and simulation results; Figs. 14, 17 and 18, respectively). There are minor differences between numerical and experimental values in the first few days, especially in the case of higher salinity (12%), but the results become identical upon further swelling.

Comparison between experimental and numerical results for bulk properties test for one case (0.6% salinity, 4 days of swelling) is given in Fig. 22. Numerical results are slightly higher than experimental ones (leading to slightly more conservative seal design), but the difference is reasonably small and the trend is the same. Over the entire 30-day swelling period (Fig. 16), there is a noticeable difference between simulation and experimental curves, though the trends are almost similar. As discussed above, reasons may include salt transport, cross-link alterations [2,4,21], or change from near-incompressible to compressible behavior.

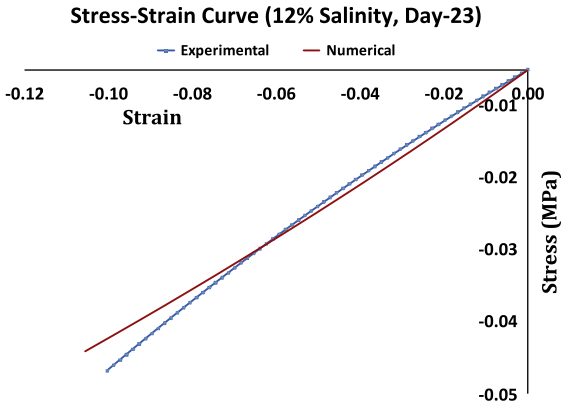

Fig. 21. Experimental and numerical stress–strain results; 12% salinity; 23 days of swelling.

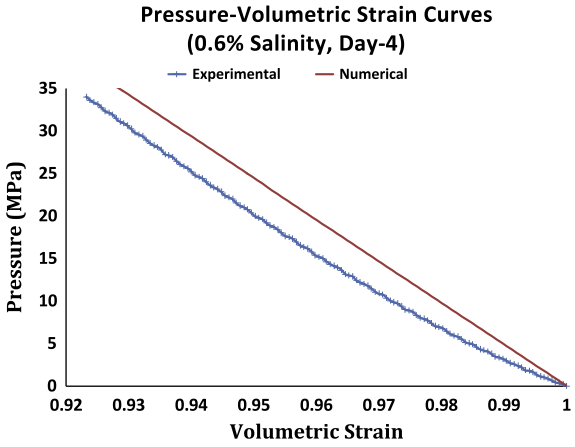

Fig. 22. Experimental and numerical pressure-strain (volumetric) results; 0.6% salinity; 4 days of swelling.

5. Conclusions

Experimental and numerical investigation of changes in compressive and bulk behavior of a water-swelling elastomer has been carried out. Major changes in both mechanical and structural properties are observed within the first two days of swelling under both salinities, agreeing well with the fast-swell nature of the elastomer. Young's and shear modulii drop to about 10% of their original value in the first week, and then show almost no variation during the remaining swelling period. Poisson's ratio exhibits the opposite trend of a sharp increase in the first few days, and then becoming almost constant with further swelling. Bulk modulus shows a fluctuating pattern, but decreases overall with swelling: relatively large initial decrease, then a somewhat slower increase, and then a much slower decrease to a nearly constant value. Salinity has almost no influence on material properties after the first week. After the first 10 days of swelling, Poisson's ratio approaches the limiting value of 0.5, providing a good justification for the assumption of incompressibility used in analytical and numerical models for rubber-like materials. Chain density decreases with swelling, sharply in the first week, and then showing almost no change. As expected, cross-link average molecular weight shows the opposite trend of an increase with swelling, but in a slightly fluctuating manner.

Salt is one of the constituents of any swelling elastomer. When exposed to saline water, some salt can enter into the elastomer material (together with absorbed water), while some salt can break away from the elastomer and go into the salt solution. Rather than a consistent increase, this two-way salt transport cause slight fluctuations in the amount of swelling. Another important factor in swelling of such elastomers is the density of cross-link chains. Salt addition and breakaway can produce breaking and later re-forming of cross-link chains, causing increase or decrease of swelling at a particular time. As both these mechanisms are dependent on salt transport, fluctuation is more significant in higher concentration brine. After some time, a sort of equilibrium is reached, inflow and outflow of salt almost balancing out, and swelling starts to show a near steady-state behavior. Slight fluctuations during the first week of swelling in the values of material and structural properties studied are due to this two-pronged variation in swelling amount. Compared to bulk tests, fluctuation is almost insignificant in compression tests due to the simple uniaxial nature of the load applied.

In general, simulation results are in good agreement with experimental ones, reinforcing the tests conducted. As testing can be costly and time-consuming, simulated values of material properties can be used for a wider range of field conditions, etc. As significant variation in material properties occurs only in the first 10 days, these values can serve as reasonable design properties for future applications, removing the need for material testing beyond 10 days of swelling. The knowledge of mechanical and structural behavior of swelling elastomer gained from this investigation can be used by oilfield engineers for selection of appropriate swelling elastomers for a given set of conditions, by development engineers to improve swell packer design, and by researchers to model and simulate elastomer seal performance.

Acknowledgments

The authors acknowledge the support of Sultan Qaboos University (SQU) and Petroleum Development Oman (PDO) for this work.

References

[1] Findik F, Yilmaz R, Köksal T. Investigation of mechanical and physical properties of several industrial rubbers. Mater Des 2004;25(4):269–76.
[2] Qamar SZ, Pervez T, Akhtar M, Al-Kharusi MSM. Design and manufacture of swell packers: influence of material behavior. Mater Manuf Processes 2012;27(7):721–6.
[3] Pervez T, Qamar SZ, van de Velden M. Comparison between fresh and exposed swelling elastomer. J Elastomers Plast 2012;44(3):237–50.
[4] Qamar SZ, Al-Hiddabi SA, Pervez T, Marketz F. Mechanical testing and characterization of a swelling elastomer. J Elastomers Plast 2009;41(5):415–31.
[5] Herold BH, Edwards JE, Kulich RV, Froehlich B, Marketz F, Welling RWF, Leuranguer C. Evaluating expandable tubular zonal and swelling elastomer isolation using wireline ultrasonic measurements. In: IADC/SPE Asia Pacific Drilling Technology Conference and Exhibition. Bangkok, Thailand; 2006.
[6] Kumar N, Marker R, Rune C, Erik GR, Statoil ASA. Mono diameter expandable drilling liner applications in deepwater drilling. In: SPE/IADC Drilling Conference and Exhibition, Paper # SPE/IADC 128175. Amsterdam, Netherlands; 2010.
[7] Campo D, Charlie W, Filippov A, Lance C, David B, Bill D, Lev R. Mono-diameter drill liner-from concept to reality. In: SPE/IADC Drilling Conference, Paper # SPE/IADC 79790. Amsterdam; 2003.
[8] Young I, Austin E, Tunde A, Adedeji O, Philip O. All-in-one concept with expandable tubular and swellable elastomer technology: a systems approach to well design. In: SPE Annual Technical Conference and Exhibition, Paper # SPE 124591. Louisiana, USA; 2009.
[9] Jay N, Sarah F, Kristaq M. Power of design: solid expandable installation sets multiple new records in deep shelf HP/HT well. In: IADC/SPE Drilling Conference, Paper # SPE/IADC 128366. Louisiana, USA; 2010.
[10] Doug G, Neven R. Expandable tubular facilitate improved well simulation and well production. In: SPE Western Regional Meeting, Paper # SPE 121147. California, USA; 2009.
[11] Robert D, Jerry F, Greg N. Combined technologies offer time-saving and efficient alternatives for zonal isolation. In: SPE Annual Technical Conference and Exhibition, Paper # SPE 125701. Bahrain; 2009.
[12] Al-Saiid KA, Abdalla E, Cherif M, Elliot SP. Practical uses of swellable packer technology to reduce water cut: case studies from the Middle East and other areas. Offshore Europe, Paper # 108613-MS. SPE Aberdeen, Scotland, UK; 2007.

[13] Thomas BR. Merging coiled tubing and swellable packer technologies. In: SPE/ICoTA Coiled Tubing & Well Intervention Conference and Exhibition, Paper # SPE 143037-MS. The Woodlands, Texas, USA; 2011.
[14] Al-Mahrooqi MA, Franz M, Ghaliba H, Improved well and reservoir management in horizontal wells using swelling elastomers. In: SPE Annual Technical Conference and Exhibition, Paper # SPE 107882-MS. Anaheim, California, USA; 2007.
[15] Glenn DD. Integrating solid expandables, swellables, and hydra jet perforating for optimized multizone fractured wellbores. In: SPE Tight Gas Completions Conference, Paper # SPE 125345-MS. San Antonio, Texas, USA; 2009.
[16] Hosford WF. Mechanical behavior of materials. Cambridge, United Kingdom: Cambridge University Press; 2005.
[17] Gent AN. Engineering with rubbers: how to design rubber components. Munich, Germany: Carl Hanser Verlag Publishers; 2012.
[18] Treloar LRG. The physics of rubber elasticity. Oxford: Oxford University Press; 2005.
[19] Ronan S, Alshuth T, Jerrams S. Long-term stress relaxation prediction for elastomers using the time–temperature superposition method. Mater Des 2007;26(5):1513–23.
[20] Aidy A, Hosseini M, Sahari BB. A review of constitutive models for rubber-like materials. Am J Eng Appl Sci 2010;3(1):232–9.
[21] Akhtar M, Qamar SZ, Pervez T, Khan R, Al-Kharusi MSM. Elastomer seals in cold expansion of petroleum tubulars: comparison of material models. Mater Manuf Processes 2012;27(7):715–20.